

# Temperature chaos, rejuvenation and memory in Migdal-Kadanoff spin glasses

M. Sasaki<sup>1</sup> and O.C. Martin<sup>2</sup>

<sup>1</sup> *Institute for Solid State Physics, University of Tokyo,  
Kashiwa-no-ha 5-1-5, Kashiwa, 277-8581, Japan*

<sup>2</sup> *Laboratoire de Physique Théorique et Modèles Statistiques,  
bât. 100, Université Paris-Sud, F-91405 Orsay, France.*

(Dated: October 31, 2018)

We use simulations within the Migdal-Kadanoff approach to probe the scales relevant for rejuvenation and memory in Ising spin glasses. First we investigate scaling laws for domain wall free energies and extract the chaos overlap length  $\ell(T, T')$ . Then we perform out of equilibrium simulations that follow experimental protocols. We find that: (1) a rejuvenation signal arises at a length scale significantly smaller than  $\ell(T, T')$ ; (2) memory survives even if equilibration goes out to length scales larger than  $\ell(T, T')$ . Theoretical justifications of these phenomena are then considered.

PACS numbers: 75.10.Nr, 05.50.+q, 75.40.Gb, 75.40.Mg

Two of the most spectacular experimental properties of spin glasses are “rejuvenation” and “memory” (see [1] and references therein). Both are out of equilibrium phenomena that arise in slowly relaxing systems [2], so understanding such properties is of great importance. Qualitatively, when a spin glass approaches equilibrium, it “ages”, reducing its susceptibility, that is its response to external perturbations. However, if one lowers the temperature after aging, one sees a restart or rejuvenation of the susceptibility, while memory of the previous aging can be retrieved upon heating back! From a theoretical point of view, rejuvenation must appear if there is “temperature chaos”, that is if the spin polarizations at two temperatures  $T$  and  $T'$  are decorrelated [3] beyond a characteristic length scale  $\ell(T, T')$ . Moreover, temperature chaos is compatible with memory through the presence of ghost domains [4]. However, temperature chaos is *not* clearly seen in Monte Carlo simulations [5, 6] and estimates of the chaos length  $\ell(T, T')$  give very large values [7], seemingly much larger than the length scale  $\ell_R$  on which rejuvenation appears experimentally.

Our purpose here is to find the scales relevant for rejuvenation and memory in Ising spin glasses. We use Migdal-Kadanoff (MK) lattices whose exact renormalization [8] allows one to measure equilibrium quantities on large *length* scales. Furthermore, it also allows for efficient dynamical simulations at very long *time* scales, enabling us to extract the length  $\ell_R$  which is relevant for rejuvenation. The outline of the paper is as follows. First, we define the MK lattices. Second we investigate *equilibrium* chaos: after extracting  $\ell(T, T')$ , we determine how the distribution of two-temperature overlaps changes with lattice size. Third, we show how (renormalized) dynamics can be used to probe rejuvenation and memory on very long length and time scales. Finally, we perform out of equilibrium measurements that follow standard experimental protocols; these signal rejuvenation even if temperature chaos is very weak and show that memory is preserved even if the equilibrated length scale is much larger than  $\ell(T, T')$ . The current theoretical frameworks

(see [9, 10] and [4]) partially account for these properties as explained in the discussion section.

*The model* — We consider MK lattices following the standard real space renormalization group approximation [8] to the Edwards Anderson (EA) model [11]. The recursive construction of such hierarchical lattices is described in Fig. 1; edges are replaced by  $2b$  edges so the “length” of the lattice is multiplied by 2. We call generation “level” the order of the recursion and  $G$  the total number of these. Then the lattice length  $L$  is  $2^G$  and the number of bonds is  $(2b)^G$  (which is also roughly the number of sites); one can thus identify  $1 + \ln b / \ln 2$  with the dimension of space on such a lattice. When all the edges are constructed, each is assigned a random coupling  $J_{ij}$ . Similarly, on each site  $i$  we put an Ising spin  $S_i = \pm 1$ . The Hamiltonian is

$$H_J(\{S_i\}) = - \sum_{\langle ij \rangle} J_{ij} S_i S_j \quad (1)$$

where the sum is over all the nearest neighbor spins of the lattice. The MK approach leads to accurate values for the spin glass stiffness exponent  $\theta$  and for the lower critical dimension; furthermore it exhibits temperature chaos [7, 12, 13]. We thus feel it is a good starting point for studying the mechanisms of rejuvenation and memory in spin glasses. All of the work presented here will be for three dimensions ( $b = 4$ ) with couplings  $J_{ij}$  taken from a Gaussian of mean 0 and width 1. The model then undergoes a spin glass transition at  $T_c \approx 0.896$  [13].

*Chaos in domain wall free energies* — Bray and Moore [3] were the first to study the temperature dependence of *domain wall* free energies. Call  $F_J^{\text{DW}}$  the free energy of a domain wall for a given disorder obtained

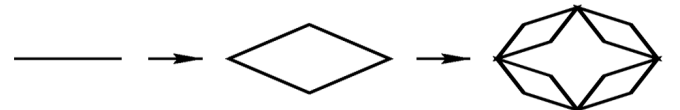


FIG. 1: Construction of a hierarchical MK lattice ( $b = 2$ ).

by forcing the outer-most spins of the MK lattice to be anti-parallel instead of parallel. ( $F_J^{\text{DW}}/2$  is the effective coupling between these spins.) When  $L$  grows,  $F_J^{\text{DW}}(T)$  and  $F_J^{\text{DW}}(T')$  become decorrelated if  $T \neq T'$ , so the linear correlation coefficient [13]

$$C^{\text{DW}}(L, T, T') = \frac{\overline{F_J^{\text{DW}}(T)F_J^{\text{DW}}(T')}}{\sigma(T)\sigma(T')} \quad (2)$$

goes to zero at large  $L$ . (In this definition,  $\overline{\quad}$  is the disorder average,  $\sigma$  is the standard deviation of  $F_J^{\text{DW}}$ , and we have used the fact that  $\overline{F_J^{\text{DW}}} = 0$ .) We are not aware of any study describing *how*  $C^{\text{DW}}$  vanishes when  $L$  grows. We thus computed  $F_J^{\text{DW}}$  for a large number of MK lattices and then estimated  $C^{\text{DW}}$ . Defining  $\ell(T, T')$  as the value of  $L$  where  $C^{\text{DW}} = 1/e$ , our data fall on a single curve when using the scaling variable  $L/\ell(T, T')$ :

$$C^{\text{DW}}(L, T, T') \sim f[L/\ell(T, T')] \quad (3)$$

This is illustrated in Fig. 2. As expected,  $\ell(T, T')$  goes as  $|T - T'|^{-1/\zeta}$  where  $\zeta$  is the chaos exponent [12]; for our system,  $\zeta = d_s/2 - \theta \approx 0.745$ . As shown in ref. [13], in the weak chaos limit  $L \ll \ell(T, T')$ ,  $1 - C^{\text{DW}} \approx [L/\ell(T, T')]^{2\zeta}$ . In the strong chaos limit,  $L \gg \ell(T, T')$ , we find that the scaling function  $f(x)$  behaves as  $\exp(-x^\alpha)$ , with  $\alpha = 1.18 \pm 0.02$ .

*The two temperature  $P(q)$*  — Beyond the length scale  $\ell(T, T')$ , domain wall free energies will often have different signs at  $T$  and  $T'$ . As a consequence, the spin orderings will be different as can be made quantitative by considering two-temperature “overlaps”. Let  $q$  be the overlap of two configurations  $\mathcal{C}$  and  $\mathcal{C}'$  taken in equilibrium (at  $T$  for  $\mathcal{C}$  and at  $T'$  for  $\mathcal{C}'$ ). Temperature chaos implies that  $P_{TT'}(q)$ , the disorder averaged distribution of such overlaps, tends towards a delta function in 0. However, this behavior has not been seen in the Sherrington-Kirkpatrick (SK) model nor in EA spin glasses [5, 6]. It is therefore interesting to see how  $P_{TT'}(q)$  behaves in MK spin glasses where temperature chaos arises for sure and  $\ell(T, T')$  is known.

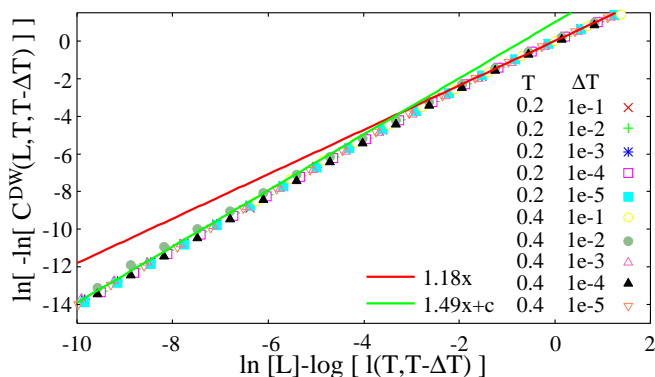


FIG. 2: Plot of  $\ln\{-\ln[C^{\text{DW}}(L, T, T - \Delta T)]\}$  to show the data collapse. The lines are the weak and strong chaos limits.

In Fig. 3 we show  $P_{TT'}(q)$  determined numerically in the case  $T = 0.7$ ,  $T' = 0.4$  for which  $\ell(T, T') = 2^{7.8}$ . When  $L = 2^G \leq 2^6$ ,  $P_{TT'}(q)$  for  $T \neq T'$  and  $T = T'$  are similar: there is a main peak at a “large” value of  $q$  and a broad tail towards lower  $q$ ; furthermore the peak position shifts to lower  $q$  with increasing  $G$ . The differences from the case  $T = T'$  are that the distributions have a shoulder and also a clear local maximum at  $q = 0$ . This behavior is close to what has been observed in the SK model [6]. Now for larger  $G$ 's, the shoulder takes over, and starting with  $G = 9$ ,  $P_{TT'}(q)$  has a single peak, located at  $q = 0$ . Note that  $G = 6$  corresponds to very large  $L$  and so the asymptotic behavior is not likely to be seen soon in the EA model.

*Exploiting renormalization for dynamical quantities* — Temperature chaos has often been used to explain rejuvenation, but temperature chaos is not necessary for rejuvenation. In particular, rejuvenation arises in generalized random energy models [14]. However, a study [10] has suggested that the influence of temperature chaos may be visible even if the domain size (or equilibrated length scale) reached experimentally is much smaller than the overlap length  $\ell(T, T')$ . Thus we ask here what is the relation between the (equilibrium) overlap length and the length scale  $l_R$  which is relevant for rejuvenation. In the framework of Migdal-Kadanoff lattices, we can address this question because one may go to long time scales as follows.

Suppose we focus on a time window  $t_{\min} \leq t \leq t_{\max}$ . Between  $t = 0$  and  $t = t_{\min}$  the system has had time to equilibrate up to the length scale  $l(t_{\min})$ ; essentially all out of equilibrium physics comes from larger length scales. On the MK lattice, this means that the spins whose generation “level” is larger than  $G_{\min}$  (with  $2^{G-G_{\min}} = l(t_{\min})$ ) are in local equilibrium; the other spins have dynamics that is well described by the effective Hamiltonian at the generation  $G_{\min}$ . In practice, we implement this idea as follows. First we generate a large number of bare couplings from a Gaussian of mean 0 and width 1. Then, we use renormalization to produce an ensemble of effective couplings. This process is iterated  $\text{NRG} \equiv G - G_{\min}$  times. (NRG is for the number of renormalization group transformations.) The final ef-

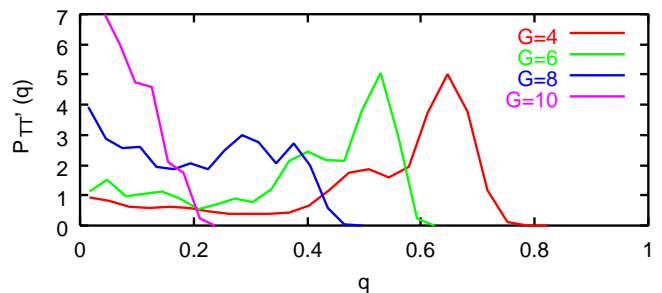


FIG. 3: Two-temperature overlap probability distribution  $P_{TT'}(q)$  when  $T = 0.7$ ,  $T' = 0.4$ ;  $L = 2^G$ .

fective couplings are then used to create a MK lattice of size  $2^{G_{\min}}$ . After that, we simply do standard Monte Carlo. Note that one Monte Carlo Sweep (MCS) on the renormalized lattice corresponds to a (huge) number of sweeps on the non-renormalized lattice, in fact to the number needed to equilibrate on the length scale  $2^{\text{NRG}}$ .

*Memory and Rejuvenation* — We use the standard temperature cycling protocol and measure a quantity similar to the ac-susceptibility defined as [15]

$$\chi(\omega, t) = \frac{1 - Q(t + \frac{2\pi}{\omega}, t)}{T} \quad (4)$$

where  $Q(t, t') \equiv \sum_i \langle S_i(t) S_i(t') \rangle / N$ . (Note that  $Q$  is a dynamical generalization of the  $q$  previously discussed.) The period  $2\pi/\omega$  of our ac-field is 16 MCS. Every MCS updates all spins once. An alternative choice is to sweep the bonds, updating their end spins as in [16]; we have checked that the results are hardly affected by the method used. The simulations were done on Migdal-Kadanoff lattices with four generations using  $0 \leq \text{NRG} \leq 15$ . In Fig. 4 we show the isothermal  $\chi$  at  $T$ , at  $T - \Delta T$ , and also  $\chi$  for a  $T \rightarrow T - \Delta T \rightarrow T$  temperature cycle. We used  $T = 0.7$  and  $\Delta T = 0.05$ . Since we calculate renormalized couplings at  $T$  and  $T - \Delta T$  from the *same* set of bare couplings, they are highly correlated when NRG is small. However, their correlation vanishes for large NRG due to temperature chaos. The direction of each spin at  $t = 0$  is chosen randomly with equal probability, corresponding to a quench from an infinitely high temperature at an infinite rate. We hereafter denote  $\chi$  with a T-cycle as  $\chi_{\text{cycle}}$  and the isothermal  $\chi$  at  $T$  as  $\chi_{\text{iso}}(T)$ .

For small NRG,  $\chi_{\text{cycle}}$  is below  $\chi_{\text{iso}}(T - \Delta T)$  in the second stage, as illustrated in Fig. 4(a). This means that the former is *older* than the latter and that equilibration is accelerated with increasing temperature; there is no rejuvenation here. On the other hand,  $\chi_{\text{cycle}}$  and  $\chi_{\text{iso}}(T)$  almost overlap in the third stage. This means that the

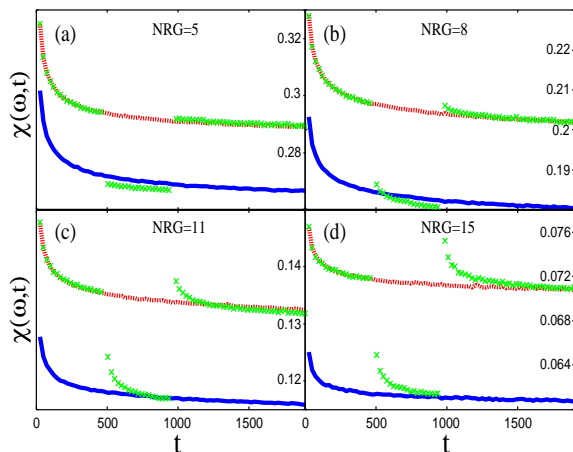


FIG. 4: Isothermal  $\chi(\omega, t)$  at  $T$  (broken line), at  $T - \Delta T$  (solid line), and  $\chi(\omega, t)$  with a negative T-cycle (crosses) for NRG = 5, 8, 11 and 15. The average is from  $10^4$  samples.

effective aging time  $t_{\text{eff}}$ , that is the equivalent time the system would have had to spend at  $T$  rather than at  $T - \Delta T$  to return to the same curve, is close to the actual window time  $t_{w2}$  spent at  $T - \Delta T$ . It is often observed in experiment that  $t_{\text{eff}}$  becomes 0 for large  $\Delta T$ , corresponding to *perfect memory*. In our simulations,  $\Delta T$  is relatively small and so we get partial memory for all NRG. This general trend of no rejuvenation yet memory with  $t_{\text{eff}} \approx t_{w2}$  arises until  $\text{NRG} \approx 7$ .

Fig. 4(b) shows that a sign of rejuvenation appears around  $\text{NRG} \approx 8$ , i.e.,  $\chi_{\text{cycle}}$  is above  $\chi_{\text{iso}}(T - \Delta T)$  at the *beginning* of the second stage. However, at later times of this second stage, the cycling curve goes *below* the  $\chi_{\text{iso}}(T - \Delta T)$  curve. The crossing of these curves has been observed experimentally [17], and will be examined in the discussion section. Finally at the beginning of the third stage, the cycling data has significant deviations from the isothermal data. The conclusion for this figure is that signs of rejuvenation emerge on smaller length scales than expected because the linear correlation coefficient is still large when  $\text{NRG} = 8$ ,  $C^{\text{DW}} = 0.965$ . ( $\ell(0.7, 0.65) \approx 2^{12}$  in this case.) This result is consistent with that in [18] where rejuvenation was observed in the 3-dimensional EA spin glass model when reversing the sign of 5% of the couplings. We have also compared  $\chi_{\text{cycle}}$  in the second stage to  $\chi_{\text{iso}}(T - \Delta T)$  shifted to the right by  $t_{w1}$ , the time of the first stage, and found that *perfect rejuvenation* (i.e., complete overlap of the two curves) arises only when  $\text{NRG} \geq 13$  where the effective couplings at the two temperatures are very decorrelated ( $C^{\text{DW}} \leq 0.10$ ).

On general grounds, one may expect  $t_{\text{eff}}$  to be smaller than  $t_{w2}$  because the temperature is lower in the second stage. However, when  $\text{NRG} = 10, 11$  and  $12$ , quite surprisingly, we find that the cycling data in the third stage are slightly *below* the isothermal data, meaning that  $t_{\text{eff}} > t_{w2}$ ; this is illustrated in Fig. 4(c).

Finally, Fig. 4(d) shows the case  $\text{NRG} = 15$ . The effective couplings at the two temperatures are now completely decorrelated. As a consequence, strong relaxation is observed not only in the second stage but also in the third stage. Now an interesting question is whether memory remains or not. We have thus compared  $\chi(\omega, t)$  in the third stage to that in the first stage, and found that the former is clearly *older* than the later. This is consistent with the prediction of ref. [4] that memory survives even if there is complete temperature chaos, i.e.,  $\ell(T, T') = 0$ .

Now for a few remarks. First, we have also performed *positive* T-cycling simulations, going from  $T = 0.7$  to  $T + \Delta T = 0.75$  in the second stage. The qualitative behavior is similar, the main difference being that equilibration is accelerated by the cycling. In particular, when NRG is not too large,  $\chi(\omega, t)$  in the third stage and at large times is below the isothermal data. This kind of behavior has been observed in glassy systems like polymer glasses [19], but not yet in spin glasses. Second, we have used the same NRG at  $T$  and  $T - \Delta T$  but really NRG should decrease with temperature because the ordering is

then slower. A temperature dependence of NRG will reduce  $t_{\text{eff}}$  which is unexpectedly large in our simulations. Moreover, it will cause separation of length scales, an important ingredient for memory and rejuvenation [20].

*Discussion and conclusions* — One of our main findings in this work is that a signal of rejuvenation arises on scales  $\ell_R$  much smaller than the equilibrium overlap length  $\ell(T, T')$ . (In Fig. 4, rejuvenation transpires even though  $\ell(T, T')/\ell_R \approx 2^4$ .) How can one interpret this result? Within the droplet picture, a small fraction of droplets of size  $l$  are fragile [3] against temperature variation even when  $l \ll \ell(T, T')$ . In our case, we equilibrate out to scales  $l_{\text{eq}}$ ; beyond  $l_{\text{eq}}$ , one has domain walls, the positions of which are time dependent and sensitive to temperature changes. The strong relaxation of  $\chi_{\text{cycle}}$  we see in the second stage can thus be interpreted as the re-ordering of the spins either inside fragile droplets or on the boundaries of the (out of equilibrium) domain walls. However, it is also possible to interpret the rejuvenation we see without appealing to temperature chaos. Indeed, in the picture of [20], there is no chaos; nevertheless, temperature cycling modifies the Boltzmann weights, leading to rejuvenation on short length scales.

A second surprising feature we found was the crossing of  $\chi_{\text{cycle}}$  and  $\chi_{\text{iso}}(T - \Delta T)$ . (See Fig. 4(b).) Interestingly, such a crossing behavior has been seen in experiments [17]. Do the different theoretical frameworks predict such a crossing? In the droplet picture, rejuvenation in Fig. 4(b) is attributed to fragile droplets. However, the equilibrium state is still robust in most regions because the occurrence of such droplets is rare at this length scale,  $l = 2^8$ . Moreover, if we compare the equilibrated length scale at  $t_{\text{w1}}$  in the T-cycling case with that in the isothermal case of  $T - \Delta T$ , the former is larger than the latter because equilibration is accelerated with increasing temperature. Therefore,  $\chi_{\text{cycle}}$  eventually goes below  $\chi_{\text{iso}}(T - \Delta T)$  after the re-ordering of fragile droplets progresses sufficiently. The picture of [20] also gives natural interpretation of the crossing. First, the positions of pinned domain walls are determined hierarchically: the structure at large scales is associated with large energies, that at small scales is associated with small energies. Second, one reaches the correct large scale structure faster by aging at  $T$  rather than at  $T - \Delta T$  since barriers are overcome more easily. (It is important that the large scale structure be the same at the two temperatures.) As a result, after transient reconstructions on smaller length scales (rejuvenation),  $\chi_{\text{cycle}}$  will cross  $\chi_{\text{iso}}(T - \Delta T)$ .

Last, our system exhibits memory which persists even when the equilibrated scale is much *larger* than  $\ell(T, T')$ . This result is completely compatible with the prediction by Yoshino *et al.* [4]. They showed that even if  $\ell(T, T') \approx 0$ , the equilibration in the second stage just injects uncorrelated short-range noise into the long-range ordering developed during the first stage; memory is then

retrieved in the third stage after transients associated with removing this noise.

We thank J.-P. Bouchaud, A. Pagnani, and E. Vincent for discussions, as well as H. Yoshino and his collaborators who have been working with a similar approach [21]. This work was partially supported by the IT-program of Ministry of Education, Culture, Sports, Science and Technology. Some of the computations were carried out on the Machikaneyama PC cluster system (URL: <http://www.mhill.org/>) in the Large-scale Computational Science Division, Cybermedia Center, Osaka University. M. S. was partially supported by the Japan Society for the Promotion of Science for Japanese Junior Scientists. M. S. acknowledges support from the MENRT while he was in France. The LPTMS is an Unité de Recherche de l'Université Paris XI associée au CNRS.

- 
- [1] V. Dupuis *et al.*, Phys. Rev. B **64**, 174204 (2001).
  - [2] L. C. E. Struik, *Physical aging in amorphous polymers and other materials*. (Elsevier, Houston, 1978).
  - [3] A. J. Bray and M. A. Moore, Phys. Rev. Lett. **58**, 57 (1987).
  - [4] H. Yoshino, A. Lemaître, and J.-P. Bouchaud, Eur. Phys. J. B. **20**, 367 (2000).
  - [5] A. Billoire and E. Marinari, J. Phys. A **33**, L265 (2000).
  - [6] A. Billoire and E. Marinari, Europhys. Lett. **60**, 775 (2002).
  - [7] T. Aspelmeier, A. Bray, and M. Moore, Phys. Rev. Lett. **89**, 197202 (2002).
  - [8] B. W. Southern and A. P. Young, J.Phys.C **10**, 2179 (1977).
  - [9] L. Berthier and J.-P. Bouchaud, Phys. Rev. B **66**, 054404 (2002).
  - [10] P. Jönsson, H. Yoshino, and P. Nordblad, Phys. Rev. Lett. **89**, 097201 (2002).
  - [11] S. F. Edwards and P. W. Anderson, J. Phys. F **5**, 965 (1975).
  - [12] J. R. Banavar and A. J. Bray, Phys. Rev. B **35**, 8888 (1987).
  - [13] M. Ney-Nifle and H. Hilhorst, Phys. Rev. Lett **68**, 2992 (1992).
  - [14] M. Sasaki and K. Nemoto, J. Phys. Soc. Jpn **69**, 2283 (2000).
  - [15] T. Komori, H. Yoshino, and H. Takayama, J. Phys. Soc. Jpn. Suppl A **69**, 228 (2000).
  - [16] F. Ricci-Tersenghi and F. Ritort, J. Phys. A **33**, 3727 (2000).
  - [17] V. Dupuis, (2002), Ph.D. Thesis, University Paris XI.
  - [18] M. Picco, F. Ricci-Tersenghi, and F. Ritort, Phys. Rev. B **63**, 174412 (2001).
  - [19] L. Bellon, S. Ciliberto, and C. Laroche, (1999), condmat/9905160.
  - [20] J.-P. Bouchaud, V. Dupuis, J. Hammann, and E. Vincent, Phys. Rev. B. **65**, 024439 (2001).
  - [21] F. Scheffler, H. Yoshino, and P. Maass, Phys. Rev. B **68**, 060404(R) (2003).